JACS
JOURNAL OF THE AMERICAN CHEMICAL SOCIETY
Article
pubs.acs.org/JACS

Overcoming Compound Fluorescence in the FLiK Screening Assay with Red-Shifted Fluorophores

Ralf Schneider,[†,⊥] Anne Gohla,[‡] Jeffrey R. Simard,[†,#] Dharmendra B. Yadav,[§,▽] Zhizhou Fang,[‡] Willem A. L. van Otterlo,[§,∥] and Daniel Rauh*[,†,‡]

[†]Chemical Genomics Centre of the Max-Planck-Society, Otto-Hahn-Strasse 15, 44137 Dortmund, Germany
[‡]Fakultät Chemie - Chemische Biologie, Technische Universität Dortmund, Otto-Hahn-Strasse 6, 44227 Dortmund, Germany
[§]Molecular Sciences Institute, School of Chemistry, University of the Witwatersrand, PO Wits, 2050, Johannesburg, South Africa
[∥]Department of Chemistry and Polymer Science, Stellenbosch University, Stellenbosch, 7602, Western Cape, South Africa

Supporting Information

ABSTRACT: In the attempt to discover novel chemical scaffolds that can modulate the activity of disease-associated enzymes, such as kinases, biochemical assays are usually deployed in high-throughput screenings. First-line assays, such as activity-based assays, often rely on fluorescent molecules by measuring a change in the total emission intensity, polarization state, or energy transfer to another fluorescent molecule. However, under certain conditions, intrinsic compound fluorescence can lead to difficult data analysis and to false-positive, as well as false-negative, hits. We have reported previously on a powerful direct binding assay called fluorescent labels in kinases ('FLiK'), which enables a sensitive measurement of conformational changes in kinases upon ligand binding. In this assay system, changes in the emission spectrum of the fluorophore acrylodan, induced by the binding of a ligand, are translated into a robust assay readout. However, under the excitation conditions of acrylodan, intrinsic compound fluorescence derived from highly conjugated compounds complicates data analysis. We therefore optimized this method by identifying novel fluorophores that excite in the far red, thereby avoiding compound fluorescence. With this advancement, even rigid compounds with multiple π-conjugated ring systems can now be measured reliably. This study was performed on three different kinase constructs with three different labeling sites, each undergoing distinct conformational changes upon ligand binding. It may therefore serve as a guideline for the establishment of novel fluorescence-based detection assays.

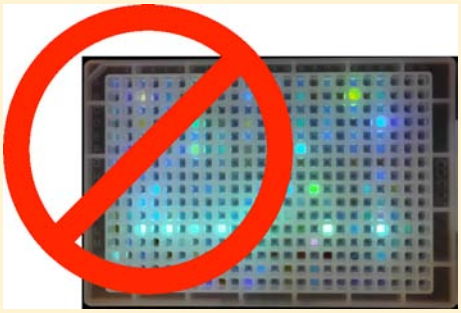

1. INTRODUCTION

High-throughput screening (HTS) of large compound libraries provides an avenue for the rapid early stage discovery of small molecules which are active against disease-associated targets. Typically, a suite of assays are developed to fully characterize hit molecules and to elucidate details of their mode of action on the target. Such an assay suite may include binding assays, enzymatic assays for the primary target, selectivity assays for secondary targets, and a variety of other biophysical and analytical methods, including surface plasmon resonance or mass spectrometry. Many of the commercially available assays rely on the use of fluorescent molecules and tags for detecting enzyme reaction products and/or monitoring the depletion of enzyme substrates. This is accomplished by measuring changes in fluorescence intensity, changes in fluorescence polarization, or by combining fluorophores to enable time-resolved Förster resonance energy transfer (TR-FRET).[1,2]

Following Lipinski's "Rule of 5" drug-like molecules usually have molecular weights ranging from 400 to 600 Da.[3,4] To achieve selectivity for the target enzyme, the chemical scaffolds of these molecules must be designed to engage in multiple interactions, such as hydrogen bonds, van der Waals forces, or $\pi-\pi$ stacking with aromatic amino acid side chains. Thus, drug-like molecules are composed of a chemical scaffold decorated with a variety of charged or uncharged moieties designed to interact with amino acids of the protein target. However, the core structures of these compounds are often rigid, planar, and composed of multiple conjugated aromatic moieties, which have a higher probability of having their own intrinsic fluorescence properties. This compound fluorescence can cause interference in fluorescence-based assay readouts, either by contributing background signal or by participating in unwanted FRET with the fluorophore(s) involved in the assay readout. Minor background fluorescence can be accounted for by measuring the fluorescence of a compound at a given concentration in the absence of all other assay components and then subtracting it from the response observed in the actual enzymatic assay.[5] However, in cases where the compound fluorescence is more intense than the fluorophore, which may occur at high compound concentrations (>10 μM), a simple subtraction of the signal may not be accurate enough. Moreover, unwanted

Received: April 8, 2013
Published: May 14, 2013

dx.doi.org/10.1021/ja403074j | J. Am. Chem. Soc. 2013, 135, 8400−8408

FRET artifacts are much more difficult to identify and to correct, leading to false-positive or -negative results. Therefore, a cascade of hit validation steps are performed after each HTS in which compounds with high intrinsic fluorescence may be lost, especially when they only have a weak affinity for the target enzyme. Such molecules, however, may be very valuable for further lead optimization, as demonstrated in fragment-based screening approaches.[6,7]

Our laboratory focuses on the development of assays for protein kinases and phosphatases, which are major classes of therapeutic targets in a variety of diseases. The dynamic, reversible phosphorylation of a target substrate protein often changes its state of activity. For the discovery of novel inhibitors which bind more favorably to inactive enzyme conformations, we have previously established detection methods called fluorescent labels in kinases ('FLiK'; Figure 1) and fluorescent labels in

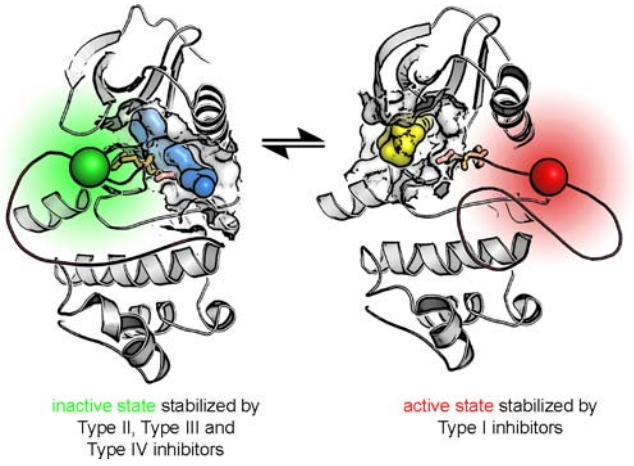

Figure 1. Principle of the FLiK assay. A thiol-reactive fluorophore is introduced at a site of the kinase which undergoes a significant conformational change upon ligand binding, thereby changing the solvent shell of the fluorophore (colored sphere), resulting in alterations in its emission spectrum. The inactive state of the kinase (left) is stabilized by a type III inhibitor (blue). Classic ATP competitive inhibitor (yellow) bound to the active kinase (right). Definition of type I–IV kinase inhibitors.[14−16]

phosphatases ('FLiP'),[8] which serve as conformation-specific binding assays for kinases and phosphatase. The FLiK assay has been established for a variety of kinases, where the environmentally sensitive fluorophore acrylodan was attached to the target kinase at a specific site which undergoes a significant conformational change upon ligand binding.[9−13] The resulting alteration of the microenvironment of acrylodan is reported by a significant change in its emission spectrum.

To date, we have used FLiK in several HTS campaigns performed both in-house[13,17] or in collaboration with pharmaceutical industry partners. In these campaigns, we have observed two challenges associated with the exclusive use of acrylodan in these assays: (i) intrinsic compound fluorescence as described above and (ii) other randomly occurring signals of high intensity ("spikes") derived from light scattering by lab dust particles. While the latter issue can be minimized by performing the HTS in a cleanroom, the problem with intrinsic compound fluorescence needed to be addressed to further improve the FLiK technology.

To do so, we conjugated eight thiol-reactive fluorophores (Table 1) to three different kinase constructs and searched for conditions where neither intrinsic compound fluorescence nor light scattering occurred. We show that an alternative fluorophore could be found for all constructs which was able to report the conformational change as reliably as acrylodan, but without the above-mentioned complications due to fluorescent compounds and light scattering. Finally, as a proof of principle, we show the value of these improvements by screening a focused library of highly rigid compounds against Abl in the FLiK assay.

2. MATERIALS AND METHODS

Recombinant kinase constructs were expressed and purified as described previously.[10−12] The fluorophores were diluted from 10 mM DMSO or DMF stock solutions to a final concentration of 15 μM in 500 μL ice-cold labeling buffer (50 mM Hepes, 200 mM NaCl, 10% glycerol, pH 7.3) before adding protein to a final concentration of 10 μM. The mixture was incubated overnight on ice in the dark. Unbound excess fluorophore was quenched with 1 mM DTT, and the protein was washed 4× in 0.5 mL centricons (Amicon Ultra-0.5, 10 kDa, Merck Millipore, Darmstadt, Germany) by concentrating down to <100 μL volumes followed by dilution to 500 μL with washing buffer (labeling buffer + 1 mM DTT). The concentrations of protein−fluorophore complexes were then determined photometrically. For this, the extinction coefficient of the protein was calculated using ProtParam (http://web.expasy.org/protparam, Swiss Institute of Bioinformatics, Lausanne, Switzerland), while the extinction coefficient of the fluorophore was determined in a dilution series (plotting the optical density at 280 nm against the fluorophore concentration). Quantitative and single labeling for all proteins was confirmed by ESI-MS (Table S1).

FLiK experiments were performed in 384 well plates as described elsewhere[10,11,17] by adding 19 μL of 100 nM protein-fluorophore conjugates diluted in FLiK buffer (50 mM Hepes, 200 mM NaCl, pH 7.4) to 1 μL of inhibitor (20x in DMSO). The final DMSO concentration in each well was 5% v/v. Fluorescence was measured on an Infinite M1000 plate reader (Tecan, Männedorf, Switzerland) as described earlier[10] and in the main text. Titrations were performed in quadruplets, Z' was determined with 8 wells of DMSO as negative control and 8 wells of 2 μM BIRB-796 + p38α or 25 μM GNF-2 + Abl, respectively, as positive control. Z' values were determined using the formula: $Z' = 1 - [3*(\sigma^p + \sigma^n)/|\mu^p - \mu^n|]$, where '$\sigma$' and '$\mu$' are the standard deviations and mean values, respectively, of the positive (p) and negative (n) controls.

3. RESULTS AND DISCUSSION

3.1. Compound Fluorescence. The initial discovery, development, and application of the FLiK approach to screening kinases in high throughput has relied so far on the fluorophore acrylodan, which has been shown to provide a very robust assay readout[9−11,13] due to the appearance of two emission maxima ($\lambda_{em,max}$) at ∼470 and ∼510 nm. When ligands bind to the labeled kinase and thereby introduce conformational changes (Figure 1), the total intensity of each of the two acrylodan emission maxima changes relative to one another, thereby enabling a highly desirable ratiometric fluorescence readout that provides a higher reliability and reproducibility when compared to monochromic readouts of intensity.[12]

This type of readout is also popular in many of the commercially available TR-FRET activity-based assays for kinases. When characterizing the labeled kinase using FLiK, the emission spectra were recorded in the presence and absence of selected kinase inhibitors which are known to induce different kinase conformations.

To determine whether compounds alone can contribute fluorescence signals at these wavelengths, thereby complicating analysis of the ratiometric readout derived from the labeled kinase, we measured the emission of compounds alone in buffer (no labeled kinase) (Figure 2a) at an initial concentration of 10

dx.doi.org/10.1021/ja403074j | J. Am. Chem. Soc. 2013, 135, 8400−8408

Table 1. Tested Fluorophores

Brand name	ΔM[c] (Da)	$\lambda_{exc,max}$[a] (nm)	$\lambda_{em,max}$[a] (nm)	QY (abs.)	Supplier	Structure
Acrylodan	225	386	470	0.18[d]	Life Technologies, Darmstadt, Germany	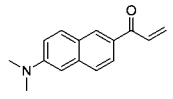
IAANS	355	326	462	1.00[e] (rel.)	Life Technologies	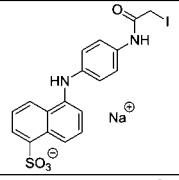
PyMPO	376	412	561	0.46[f] (rel.)	Life Technologies	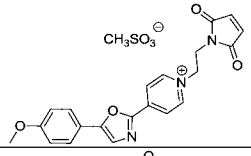
Texas Red C2	729	595	615	0.09[g] (rel.)	Life Technologies	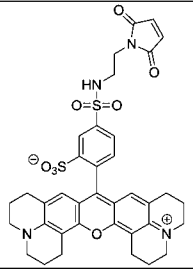
Alexa Fluor 660[b]	~ 900	663	690	0.37[h]	Life Technologies	structure not provided by supplier
DY-647	764	653	672	0.26[h]	Dyomics, Jena, Germany	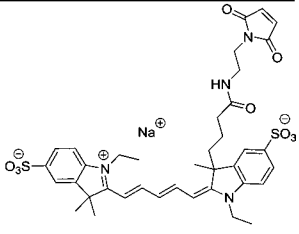
Atto 565	634	563	592	0.90[h]	Atto-Tec, Siegen, Germany	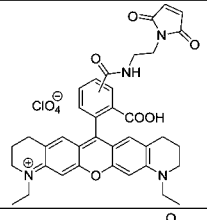
Atto 610	514	615	634	0.70[h]	Atto-Tec	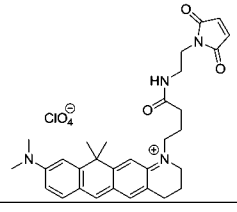

[a]Excitation and emission maxima as provided by the supplier. [b]Neither structure nor exact molecular mass of Alexa Fluor 660 was provided by the supplier. [c]Δ*M*: Mass increase after reaction with protein. [d]QY of acrylodan-mercaptoethanol adduct in water.[18] [e]cTnC mutant labeled with IAANS at Cys-84; QY in EGTA buffer using quinine sulfate in 0.1 N H_2SO_4 as standard (0.52 at λ_{ex} = 365 nm and 0.47 at λ_{ex} = 325 nm).[19] [f]QY in water (pH 1.0) using quinine sulfate in 5 M H_2SO_4 as standard (QY = 0.55).[20] [g]Texas Red-transferrin conjugate in aqueous solution using sulforhodamine 101 as standard.[21] [h]Determined in aqueous buffer solution as provided by the supplier.

μM, which is a typical compound concentration used in HTS campaigns.[1] Compounds with extensive π−electron systems, such as staurosporine and especially DBY-14 (a highly rigid analog of the allosteric Abl ligand GNF-2 synthesized in-house), displayed strong intrinsic emission up to 450 nm when excited at the excitation maximum for acrylodan (386 nm). Next, we

dx.doi.org/10.1021/ja403074j | J. Am. Chem. Soc. 2013, 135, 8400−8408

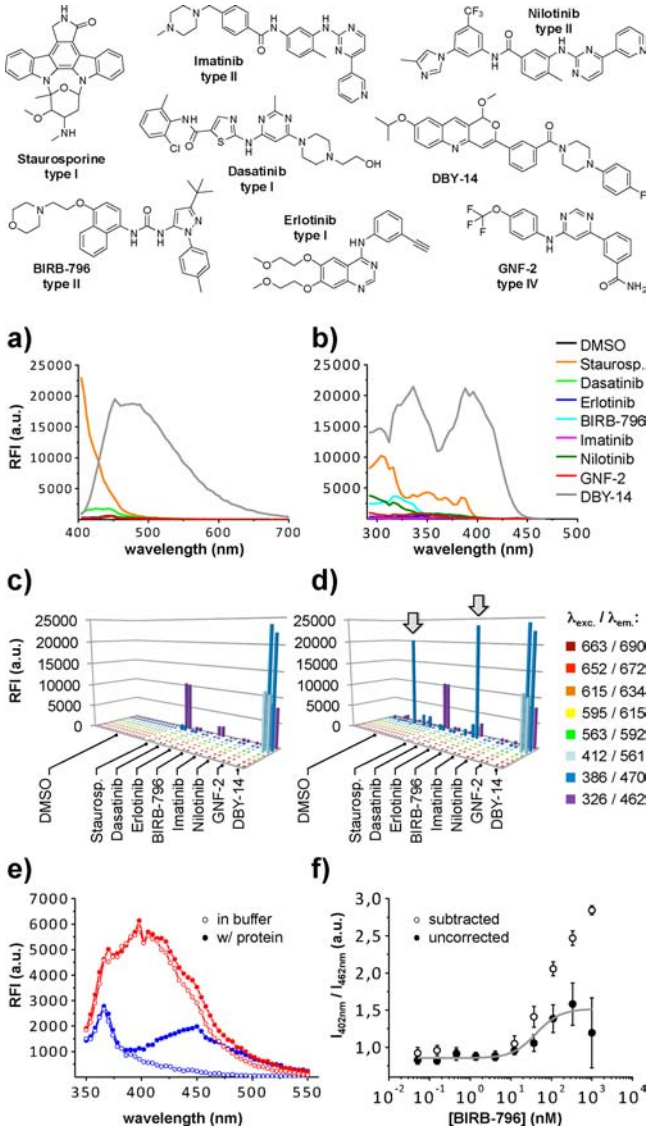

Figure 2. Effects of compound fluorescence. (a) Emission spectra of 10 μM compounds in FLiK buffer (λ_{exc} = 386 nm). (b) Excitation spectra (λ_{em} = 500 nm). (c) Emission of 10 μM compounds in FLiK buffer with λ_{exc} and λ_{em} as provided by the supplier. Measuring under the settings for IAANS (purple), acrylodan (dark blue), and PyMPO (light blue) resulted in intrinsic fluorescence of rigid inhibitors. No intrinsic compound fluorescence is observed under the settings for the remaining fluorophores. (d) Rubbing the plate once on a lab coat to simulate a dusty lab environment generated new fluorescent signals with high intensity under the acrylodan settings (arrows), demonstrating sensitivity to lab dust. (e) Emission spectra of p38α labeled with IAANS at the activation loop (filled circles) in the apo form (blue) and supplemented with 1 μM BIRB-796 (red). Most of the fluorescence is derived from the compound (open circles). (f) Ratiometric fluorescence ($R = I_{402\ nm}/I_{462\ nm}$) without (filled circles) and with subtraction of the background fluorescence (filled circles) plotted against the inhibitor concentration. RFI is relative fluorescence intensity, and a.u. is arbitrary units.

recorded the excitation spectra of these inhibitors to determine the shortest wavelength at which these compounds will not produce an emission signal (Figure 2b). Less complex compounds, such as imitinib or GNF-2, which only have single aromatic ring systems, were not significantly excitable at wavelengths above ~300 nm, while compounds with a two-ring conjugated system, such as erlotinib or BIRB-796 were excitable up to ~350 nm. Compounds with multiple conjugated ring systems (>2 rings), such as staurosporine, were excitable at much higher wavelengths. Notably, above 450 nm, none of the chosen compounds were excitable. We therefore conclude that fluorophores with an absorption (λ_{exc}) at >450 nm would likely reduce the occurrence of intrinsic compound fluorescence and might be chosen as alternatives for acrylodan to develop a far-red FLiK assay.

Thus, a mixture of five commercially available fluorophores (Atto 565, Texas Red, Atto 610, Dy-647, and Alexa Fluor 660) was selected, which all have excitation maxima well above 450 nm. Additionally, we investigated PyMPO, which has an excitation maximum between 400 and 450 nm, and compared their performance to the fluorophores IAANS and acrylodan, which excite at lower wavelengths (<400 nm) (Table 1).

As mentioned above, the FLiK assays developed to date by our laboratory were at risk for a higher rate of detection of false positives due to intrinsic compound fluorescence. Many of these false positives were due to additive fluorescence signal coming from the compounds at the emission wavelengths being monitored in a particular assay. We were able to minimize the number of such false-positives by subtracting their intrinsic fluorescence (as measured in buffer) from the total fluorescence intensity (obtained when the compound is placed into solution with the labeled kinase).[5] However, FRET-based fluorescence artifacts due to energy transfer between compound and fluorophore are not additive and can still lead to false-positives or false-negatives. Data derived from such compounds are significantly more difficult to analyze.

In an attempt to avoid such unwanted interactions between the chosen fluorophore and these compounds, it became necessary to investigate the performance of fluorophores which excite at longer wavelengths. As done for acrylodan, we measured 10 μM solutions of the reference inhibitors in buffer using the excitation and emission wavelengths (λ_{exc}, λ_{em}, respectively) provided by the supplier for the different fluorophores (Figure 2c). When using λ_{exc} and λ_{em} reported for IAANS, we measured significant intrinsic compound fluorescence for staurosporine, DBY-14, and BIRB-796, and, with much reduced intensity, dasatinib, nilotinib, and GNF-2. Under the acrylodan conditions, less rigid molecules, such as BIRB-796 or GNF-2, did not show significant intrinsic fluorescence any more as expected from Figure 2b, but DBY-14 showed an extremely high intrinsic fluorescence. When excited at 412 nm (PyMPO), only DBY-14 was fluorescent, while all other inhibitors were not detected. Notably, when excited at >450 nm, no intrinsic fluorescence could be observed for any molecule, confirming that the use of far-red fluorophores allows for the measurement of highly conjugated molecules.

We then simulated a dusty lab environment by striking the assay plates on a standard white cotton lab coat. Several spikes suddenly appeared (Figure 2d) under the acrylodan settings. Similar effects were observed under the IAANS settings but with much reduced intensity. Notably, these added spikes did not appear under any other conditions tested, suggesting that the lab dust particles would not have an effect when using fluorophores that absorb at >400 nm.

Finally, to investigate how these alternative fluorophores would perform in an assay setting, we analyzed data obtained from three recombinant kinase constructs labeled on three different structural features of the kinase domain that undergo significant conformational changes upon ligand binding. In these

dx.doi.org/10.1021/ja403074j | J. Am. Chem. Soc. 2013, 135, 8400−8408

constructs, the fluorophores were fused by nucleophilic substitution (IAANS) or Michael addition (all other fluorophores) to (i) the activation loop ('a-loop') of p38α, (ii) the glycine-rich loop ('p-loop') of p38α, and (iii) the myristate pocket of Abl, as described previously[10−12] and in Materials and Methods.

3.2. Labeling at the Activation Loop of p38α. The negative effect of intrinsic compound fluorescence on the assay readout of FLiK could easily be demonstrated using p38α labeled with IAANS at the a-loop. BIRB-796, a potent type II inhibitor of p38α, displayed moderate levels of intrinsic compound fluorescence in FLiK buffer when excited at 326 nm (Figure 2c), the excitation maximum for IAANS. The emission spectra of IAANS-labeled p38α (a-loop) obtained in the presence and absence of 1 μM BIRB-796 (Figure 2e) showed a significant left-shift of the emission maximum from ~460 nm (apo) to 402 nm (1 μM BIRB-796). However, by overlaying spectra of BIRB-796 recorded with (filled circles) or without (open circles) labeled protein, it is clear that most of the recorded fluorescence at 402 nm is derived from the compound rather than the attached fluorophore. Nevertheless, plotting the ratio of emission intensities at 402 and 462 nm measured with protein against the logarithmic inhibitor concentration (Figure 2f) generates a nearly sigmoidal regression curve. However, the standard deviations became very large at high compound concentrations, further suggesting the influence of background fluorescence on these ratiometric values. Performing a background correction (by subtracting the intensity measured in buffer from the one measured with protein at each inhibitor concentration) leads to a significantly different regression curve, further demonstrating that this fluorophore is not suitable for FLiK.

Using a-loop labeled p38α, the same procedure was used to investigate the suitability of the remaining fluorophores, in this case using acrylodan as the reference fluorophore having the lowest excitation maximum of the collection (Figure 3). Interestingly, no intrinsic fluorescence was observed up to a concentration of 10 μM BIRB-796 for all of the remaining fluorophores tested (see Figure 2c), suggesting that background correction would not be necessary when using these fluorophores.

For each kinase-fluorophore conjugate, the emission spectrum of p38α labeled at the a-loop with each different fluorophore was recorded in its unbound (apo) state to identify the emission maxima suitable for calculating a ratiometric readout for detecting the binding of BIRB-796 (Figure 3a). Spectra recorded under BIRB-saturated conditions were then overlaid to identify secondary emission wavelengths to calculate ratiometric readouts with an internal calibration. This secondary emission wavelength was easily identified in the spectrum of acrylodan, which exhibits different maxima in the bound and unbound states.[11] Also, PyMPO showed a significant bathochromic shift, however smaller as compared to acrylodan. For all other fluorophores tested, we selected a secondary wavelength at a shoulder of the main peak (Texas Red, Alexa Fluor 660, Dy-647, Atto 565) and/or where the emission was stable and did not change emission intensity significantly upon ligand binding (Dy-647, Atto 610). In either case, one wavelength changes significantly relative to another, resulting in a ratiometric fluorescence change associated with ligand binding.

Plotting the ratiometric fluorescence against the logarithmic concentration of BIRB-796 resulted in sigmoidal regression curves with all fluorophores except Atto 565, where no change in the ratio was observed under the chosen conditions. This

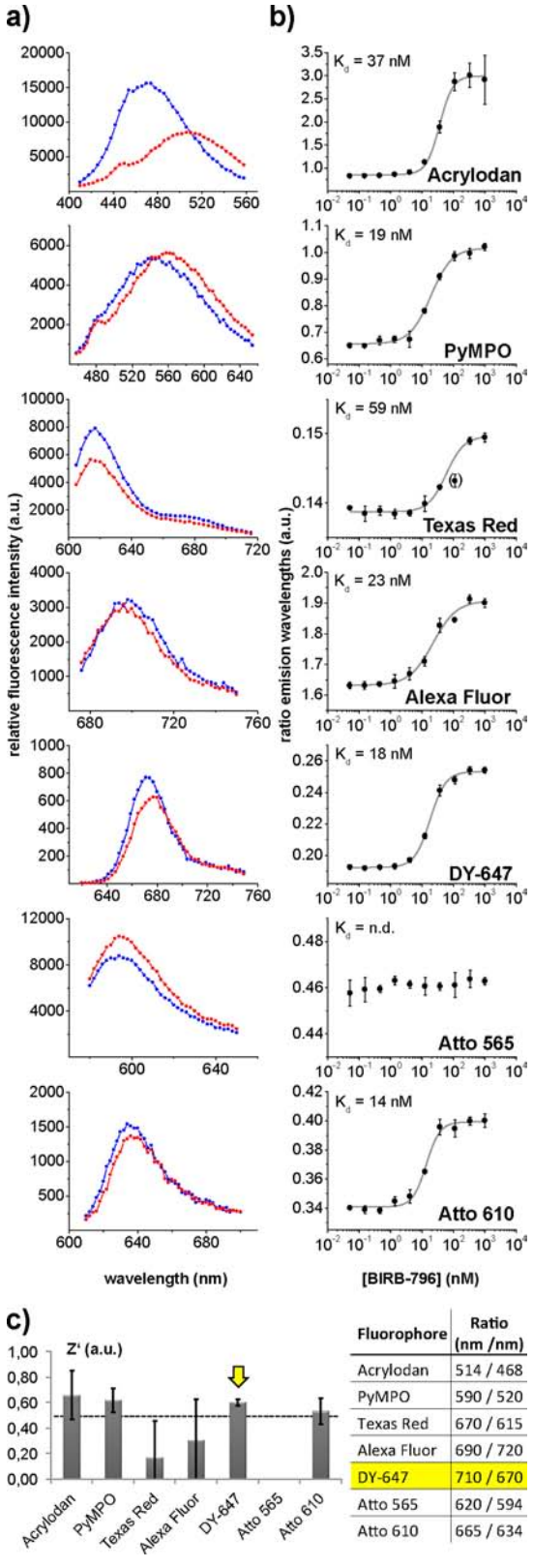

Fluorophore	Ratio (nm /nm)
Acrylodan	514 / 468
PyMPO	590 / 520
Texas Red	670 / 615
Alexa Fluor	690 / 720
DY-647	710 / 670
Atto 565	620 / 594
Atto 610	665 / 634

Figure 3. Emission spectra and titration curves of p38α labeled at the a-loop. (a) Emission spectra recorded in the absence (blue) and presence (red) of 1.7 μM BIRB-796. (b) Titration curves of the protein-fluorophore conjugates. The ratiometric assay readout for each fluorophore is summarized in the table below. (c) Calculated Z' factors (n = 3). Arrow: best alternative for acrylodan.

dx.doi.org/10.1021/ja403074j | J. Am. Chem. Soc. 2013, 135, 8400−8408

fluorophore is therefore unable to report the conformational change associated with movement of the activation loop of p38α. The K_d values for BIRB-796 determined from the regression curves of the other fluorophores were within 2-fold of our previously reported K_d value for BIRB-796 (30 nM).[17] Although most fluorophores could report affinity, the assay window (maximal ratio change) and reproducibility varied. Calculating the Z', a commonly used factor describing the robustness of an assay,[2] we found that PyMPO and Dy-647 worked as well as the reference fluorophore (acrylodan). Notably, Dy-647 displayed the lowest standard deviation ($n = 3$) (Figure 3c) and, in contrast to PyMPO, no sensitivity toward interference from compound fluorescence (Figure 2b,c).

These findings suggest that the use of Dy-647 may enable more straightforward detection of highly conjugated and rigid compounds (Figure 2a,c) which have high intrinsic fluorescence when excited at lower wavelenths. Thus, to reduce the number of false hits picked up in HTS FLiK screens, we propose that Dy-647 would serve as a suitable alternative to acrylodan. In fact, when applied to the a-loop of p38α, selectivity for type II and III inhibitors was observed for this fluorophore (Figure S1a), as previously described with acrylodan.[12] Additionally, type IV allosteric inhibitors binding to the remote p38α MAP insert pocket[9] were not detected, further suggesting that Dy-647 is amenable for HTS campaigns and retains the expected selective detection of ligands which trigger conformational changes in the a-loop.

3.2. Labeling at the Glycine-Rich Loop of p38α. We took a similar approach to study p38α labeled on the glycine-rich loop, a FLiK assay designed to detect the binding of type I (DFG-in conformation) as well as types II and III (DFG-out) inhibitors without relying on activity-based assays.[11] Similar experiments were carried out as described above for the a-loop FLiK assay. In this case, three fluorophores (Texas Red, Dy-647, and Atto565) were unable to report the conformational change upon binding of the reference inhibitor BIRB-796 (Figure 4a,b) under the chosen conditions. Besides acrylodan, PyMPO, and Atto 610 provided the best assay performance, as judged by the Z' factor (Figure 4c). The spectral changes were the greatest in the case of PyMPO, but again due to the possibility of inducing unwanted compound fluorescence at wavelengths used to excite PyMPO (see Figure 2b,c), Atto 610 was chosen as the best alternative for acrylodan in this protein construct. With Atto 610, a clear bathochromic shift (arrow in Figure 4a) was observed in the emission spectra when a saturating amount of inhibitor was added. This shift indicates a change in the solvent shell of the fluorophore[22] due to an increased exposure to the buffer as a result of the conformational change around the labeling site. As expected for the p-loop as labeling site,[11] types I–III, but not type IV, inhibitors were detected using this fluorophore (Figure S1b).

3.3. Labeling at the Myristate Pocket of Abl. Finally, we tested alternative fluorophores with Abl labeled at the myristate pocket as a representative FLiK assay for a remote allosteric binding site residing outside of the ATP binding cleft. We labeled Abl in a manner which allows detection of conformational changes in helix I at the C-terminal end of the kinase domain.[10] Upon addition of 30 μM GNF-2, a known type IV Abl inhibitor, only minor changes in the spectra of Abl kinase labeled with PyMPO, Texas Red, or Dy-647 were observed (Figure 5a). This translated into a weak or unmeasurable Z' for these three fluorophore-Abl conjugates (Figure 5c). By stark contrast, Atto 565 exhibited the largest bathochromic shift in the emission spectra upon binding of GNF-2 when compared to the remaining

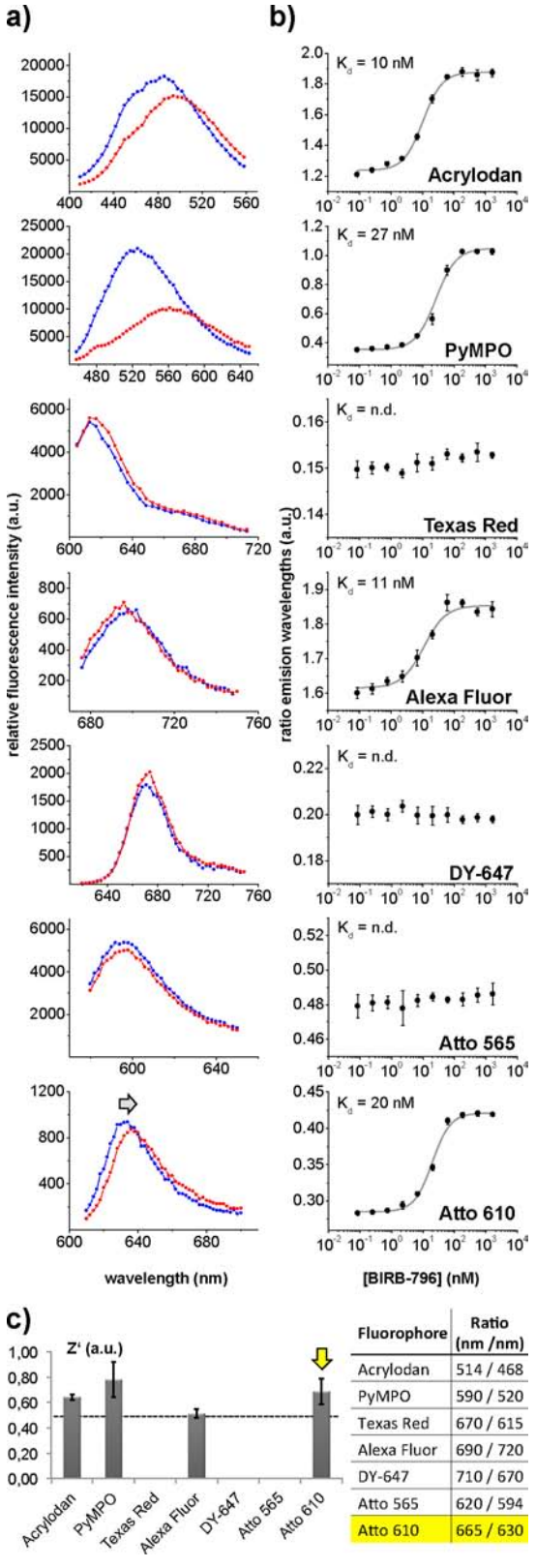

Fluorophore	Ratio (nm /nm)
Acrylodan	514 / 468
PyMPO	590 / 520
Texas Red	670 / 615
Alexa Fluor	690 / 720
DY-647	710 / 670
Atto 565	620 / 594
Atto 610	665 / 630

Figure 4. Emission spectra and titration curves of p38α labeled at the glycine-rich loop. (a–c) Description as in Figure 3.

fluorophores. With Atto 565, an excellent signal-to-noise ratio was obtained together with small standard deviations of each data point (Figure 5b), resulting in the strongest Z' of this collection of fluorophores. The quality of this FLiK assay was comparable to

dx.doi.org/10.1021/ja403074j | J. Am. Chem. Soc. 2013, 135, 8400–8408

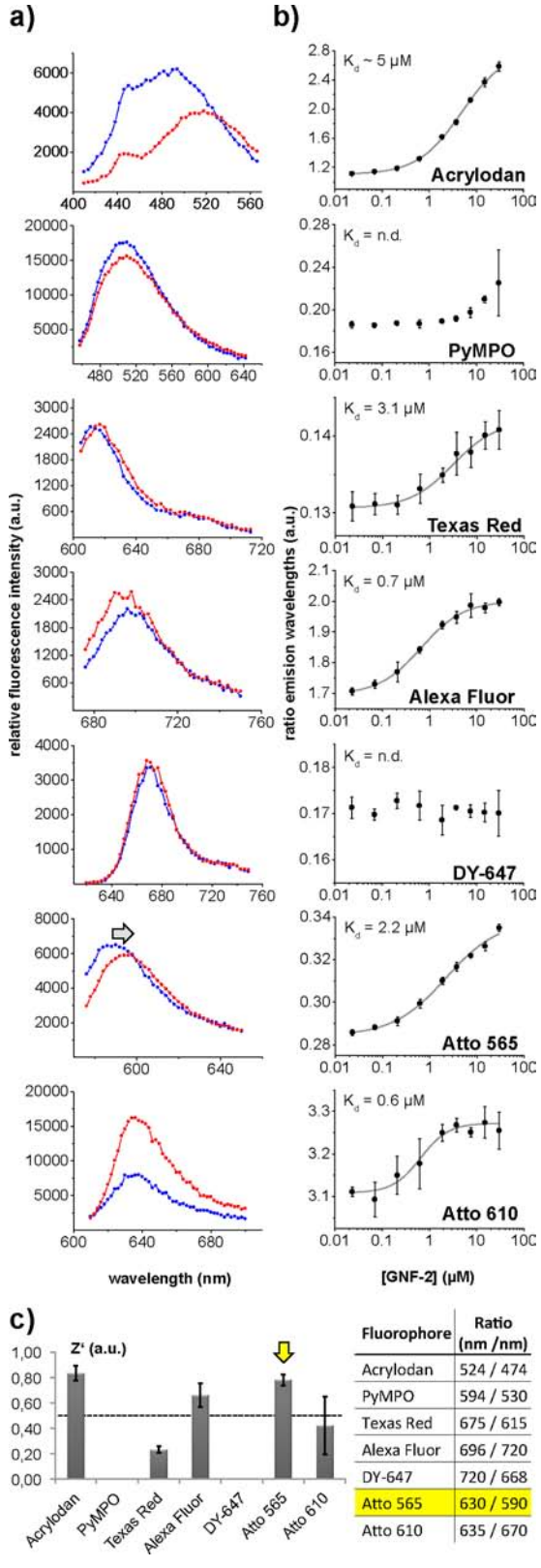

Fluorophore	Ratio (nm /nm)
Acrylodan	524 / 474
PyMPO	594 / 530
Texas Red	675 / 615
Alexa Fluor	696 / 720
DY-647	720 / 668
Atto 565	630 / 590
Atto 610	635 / 670

Figure 5. (a) Emission spectra (blue: apo; red: +30 μM GNF2) and (b) titration curves of Abl labeled at the myristate pocket. (c) Calculated Z'. Due to limited solubility of GNF-2 in buffer,[24] the titrations did not exceed 30 μM.

the one previously developed with acrylodan-labeled Abl (Figure 5c).

The assay window could be further increased by calculating the ratio of the fluorescence measured to the right of the maximum (610 nm) and left to the maximum (576 nm) (Figure S1c), since the intensities at these two wavelengths moved in opposite directions upon binding (Figure 5a). Titration of Abl-Atto 565 with allosteric activators (DPH) and inhibitors (GNF-2) gave sigmoidal regression curves with K_d values in the expected range,[10,23] while types I and II (i.e., ATP competitive) inhibitors were not detected (Figure S1c), further suggesting this FLiK assay as a robust tool for the discovery of novel allosteric ligands of Abl.

Having identified a far-red-shifted fluorophore that was compatible with a FLiK assay for the myristate pocket of Abl, it was possible to perform screens under conditions which would minimize the detection of highly fluorescent GNF-2 analogs. We synthesized a small library of rigid GNF-2 analogs which we tested with the old (acrylodan) and new (Atto 565) Abl FLiK assay. We first recorded the emission spectra of these compounds alone (10 μM) using the emission and excitation wavelengths for either acrylodan or Atto 565 (Figure 6a). When excited at 386 nm (λ_{exc} of acrylodan), severe compound fluorescence was measured that saturated the detector for several of these compounds (DBY-10−16, 18−21, 23), therefore disabling them from ratiometric measurement. For the remaining compounds, intrinsic fluorescence was observed, but it did not reach saturated levels.

When using acrylodan, uncorrected and background corrected ratiometric data are significantly different (Figure 6b), suggesting that the majority of the detected signal is derived from the compound alone. Additionally, standard deviations (n = 2) were high in the background corrected data set, which indicates low reliability of the assay readout. In our previous screens, we excluded such compounds with background fluorescence >3× the signal for DMSO alone, meaning that all DBY compounds would have been excluded during the hit evaluation despite being close analogs of GNF-2, a known ligand of the allosteric Abl site.

These issues were all avoided by switching to Abl-Atto 565, demonstrating the great advantage of using this far-red-shifted fluorophore. The lack of compound interference (Figure 6a) becomes more apparent when comparing corrected and uncorrected fluorescence data (Figure 6c). Unlike with acrylodan-labeled Abl, the corrected and uncorrected values obtained with Abl-Atto 565 were practically identical, and the ratiometric data for all compounds could be calculated reliably. Thus, using Atto 565 circumvents the problem of intrinsic fluorescence with this particular class of compounds and would enable their characterization in the Abl FLiK assay.

4. DISCUSSION AND SUMMARY

We have shown the importance of using fluorophores that are excitable at >450 nm to avoid intrinsic compound fluorescence. Light scattering is also avoided, further reducing the number of putative false-positive and -negative hits picked up during screening scenarios.

We showed the general applicability of red-shifted fluorophores by fusing eight different fluorophores to three different kinase constructs, each labeled on structural elements that undergo significant and distinct conformational changes. For all protein-fluorophore conjugates tested, alternative fluorophores were identified which can report this conformational change as reliably as acrylodan, the original fluorophore used in the development of these various FLiK assays. With these red-shifted fluorophores, even highly rigid compounds with high intrinsic

dx.doi.org/10.1021/ja403074j | J. Am. Chem. Soc. 2013, 135, 8400−8408

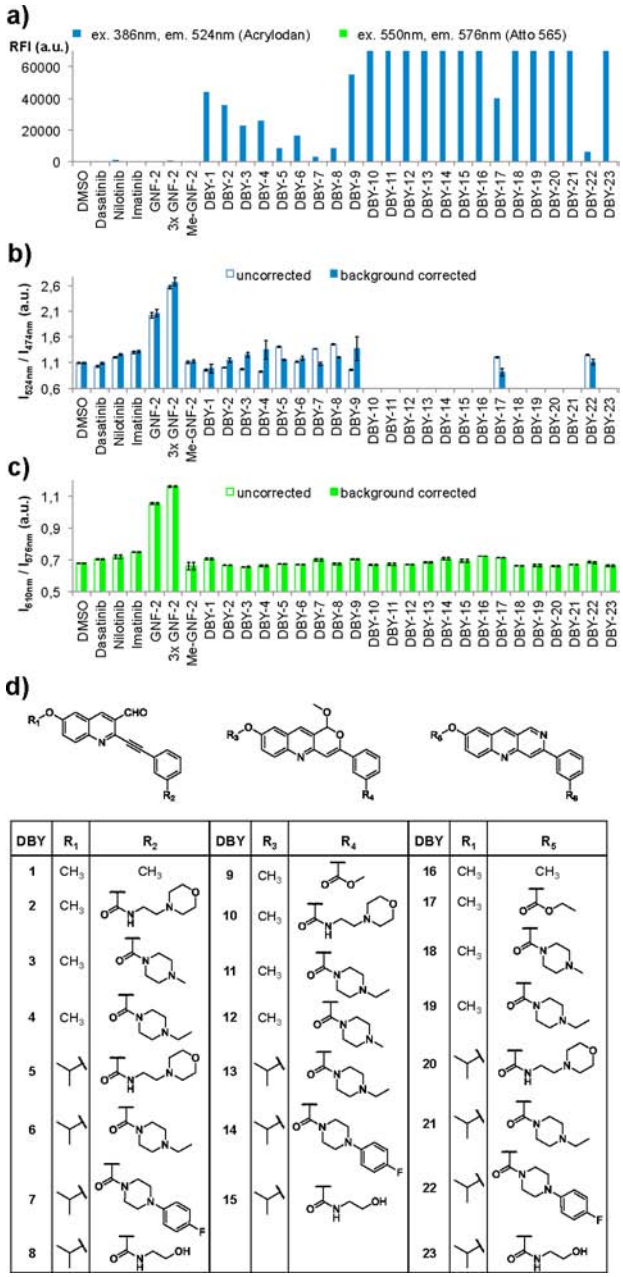

Figure 6. Screen of rigid GNF-2 analogs. (a) High intrinsic fluorescence (10 μM DBY compounds in FLiK buffer) is observed under the acrylodan settings (blue), while no interference was observed under the Atto 565 settings (green). (b,c) Ratiometric assay readout of Abl labeled with acrylodan (b) and Atto 565 (c) supplemented with 10 μM DBY compounds ($n = 2$). (d) Structures of the analyzed compounds (see also Figure 2).

compound fluorescence (as recorded at lower wavelengths) could now be reliably measured.

In general, the best assay performance was achieved when a bathochromic shift was detected upon ligand binding, as seen in the case of Abl labeled with Atto 565. Calculating a ratio of intensities measured left and right to the shifting maximum allows for a straightforward detection of ligand binding. A simple intensity decrease of the emission maxima without a bathochromic shift, as, for example, seen with p38α labeled with Texas Red at the a-loop, translated into poor assay performance. Even a minor bathochromic shift of only a few nanometers, as seen with p38α labeled with Atto 610 at the a-loop, can translate into a robust assay as judged by the Z' factor.

These results represent a major improvement of our FLiK technology that will enable a more straightforward discovery of complex enzyme inhibitors and reduce the number of fluorescence artifacts and false positives and negatives. Furthermore, it is a valuable starting point for the development of more red-shifted fluorescence-based assays detecting conformational changes in a target enzyme without relying on activity measurements. This study may therefore be especially interesting to be applied in assays for ligands of allosteric binding sites which are modulated by conformational changes and where conventional assays fall short.

■ ASSOCIATED CONTENT

Ⓢ Supporting Information

Table S1 and Figure S1. This material is available free of charge via the Internet at http://pubs.acs.org.

■ AUTHOR INFORMATION

Corresponding Author

daniel.rauh@tu-dortmund.de

Present Addresses

[⊥]Sartorius Stedim Biotech GmbH, August-Spindler-Str. 11, 37079 Göttingen, Germany.
[#]Amgen Inc., 360 Binney St., Cambridge, MA 02142, U.S.A.
[▽]Curadev Pharma Pvt. Ltd., B-87, Sector 83, Noida, India.

Notes

The authors declare no competing financial interest.

■ ACKNOWLEDGMENTS

We thank Prof. Charles B. de Koning (School of Chemistry, University of the Witwatersrand, Johannesburg) for synthetic advice, Ms. Simone Eppmann (Dortmund) for protein preparation, and Mr. André Richters (Dortmund) for helpful discussions. This work was cofunded by the German federal state North Rhine Westphalia (NRW) and the European Union (European Regional Development Fund: Investing In Your Future), the German Federal Ministry for Education and Research (NGFNPlus) (grant no. BMBF 01GS08104) all to D.R. D.B.Y. and W.A.L.v.O acknowledge the National Research Foundation, Pretoria, South Africa for research funding and the University of the Witwatersrand Research Office for postdoctoral funding for D.B.Y.

■ REFERENCES

(1) Macarron, R.; Hertzberg, R. P. *Mol. Biotechnol.* **2009**, *47*, 270.
(2) Inglese, J.; Johnson, R. L.; Simeonov, A.; Xia, M.; Zheng, W.; Austin, C. P.; Auld, D. S. *Nat. Chem. Biol.* **2007**, *3*, 466.
(3) Lipinski, C. A.; Lombardo, F.; Dominy, B. W.; Feeney, P. J. *Adv. Drug Delivery Rev.* **2001**, *46*, 3.
(4) Anastassiadis, T.; Deacon, S. W.; Devarajan, K.; Ma, H.; Peterson, J. R. *Nat. Biotechnol.* **2011**, *29*, 1039.
(5) Simard, J. R.; Rauh, D. *Methods Mol. Biol.* **2012**, *800*, 95.
(6) Murray, C. W.; Rees, D. C. *Nat. Chem.* **2009**, *1*, 187.
(7) Erlanson, D. A. *Top. Curr. Chem.* **2012**, *317*, 1.
(8) Schneider, R.; Beumer, C.; Simard, J. R.; Grütter, C.; Rauh, D. *J. Am. Chem. Soc.* **2013**, *135*, 6838.
(9) Getlik, M.; Simard, J. R.; Termathe, M.; Grütter, C.; Rabiller, M.; van Otterlo, W. A.; Rauh, D. *PloS one* **2012**, *7*, e39713.
(10) Schneider, R.; Becker, C.; Simard, J. R.; Getlik, M.; Bohlke, N.; Janning, P.; Rauh, D. *J. Am. Chem. Soc.* **2012**, *134*, 9138.
(11) Simard, J. R.; Getlik, M.; Grütter, C.; Schneider, R.; Wulfert, S.; Rauh, D. *J. Am. Chem. Soc.* **2010**, *132*, 4152.

(12) Simard, J. R.; Getlik, M.; Grütter, C.; Pawar, V.; Wulfert, S.; Rabiller, M.; Rauh, D. *J. Am. Chem. Soc.* **2009**, *131*, 13286.
(13) Simard, J. R.; Klüter, S.; Grütter, C.; Getlik, M.; Rabiller, M.; Rode, H. B.; Rauh, D. *Nat. Chem. Biol* **2009**, *5*, 394.
(14) Rabiller, M.; Getlik, M.; Klüter, S.; Richters, A.; Tückmantel, S.; Simard, J. R.; Rauh, D. *Arch. Pharm.* **2010**, *343*, 193.
(15) Fang, Z.; Grütter, C.; Rauh, D. *ACS Chem. Biol.* **2013**, *8*, 58.
(16) Dar, A. C.; Shokat, K. M. *Annu. Rev. Biochem.* **2011**, *80*, 769.
(17) Simard, J. R.; Grütter, C.; Pawar, V.; Aust, B.; Wolf, A.; Rabiller, M.; Wulfert, S.; Robubi, A.; Klüter, S.; Ottmann, C.; Rauh, D. *J. Am. Chem. Soc.* **2009**, *131*, 18478.
(18) Prendergast, F. G.; Meyer, M.; Carlson, G. L.; Iida, S.; Potter, J. D. *J. Biol. Chem.* **1983**, *258*, 7541.
(19) Dong, W. J.; Wang, C. K.; Gordon, A. M.; Cheung, H. C. *Biophys. J.* **1997**, *72*, 850.
(20) Diwu, Z.; Chen, C. S.; Zhang, C.; Klaubert, D. H.; Haugland, R. P. *Chem. Biol.* **1999**, *6*, 411.
(21) Panchuk-Voloshina, N.; Haugland, R. P.; Bishop-Stewart, J.; Bhalgat, M. K.; Millard, P. J.; Mao, F.; Leung, W. Y. *J. Histochem. Cytochem.* **1999**, *47*, 1179.
(22) Lakowicz, J. R. *Principles of Fluorescence Spectroscopy*; Springer: New York, 2006; Vol. 3.
(23) Yang, J.; Campobasso, N.; Biju, M. P.; Fisher, K.; Pan, X. Q.; Cottom, J.; Galbraith, S.; Ho, T.; Zhang, H.; Hong, X.; Ward, P.; Hofmann, G.; Siegfried, B.; Zappacosta, F.; Washio, Y.; Cao, P.; Qu, J.; Bertrand, S.; Wang, D. Y.; Head, M. S.; Li, H.; Moores, S.; Lai, Z.; Johanson, K.; Burton, G.; Erickson-Miller, C.; Simpson, G.; Tummino, P.; Copeland, R. A.; Oliff, A. *Chem. Biol.* **2011**, *18*, 177.
(24) Zhang, J.; Adrian, F. J.; Jahnke, W.; Cowan-Jacob, S. W.; Li, A. G.; Iacob, R. E.; Sim, T.; Powers, J.; Dierks, C.; Sun, F.; Guo, G. R.; Ding, Q.; Okram, B.; Choi, Y.; Wojciechowski, A.; Deng, X.; Liu, G.; Fendrich, G.; Strauss, A.; Vajpai, N.; Grzesiek, S.; Tuntland, T.; Liu, Y.; Bursulaya, B.; Azam, M.; Manley, P. W.; Engen, J. R.; Daley, G. Q.; Warmuth, M.; Gray, N. S. *Nature* **2010**, *463*, 501.